JOURNAL OF PROPULSION AND POWER
Vol. 14, No. 5, September–October 1998

Experimental Performance of Field Emission Microthrusters

Salvo Marcuccio,* Angelo Genovese,† and Mariano Andrenucci‡
Centrospazio, Ospedaletto 56014, Pisa, Italy

This paper presents the results of a series of tests performed on a set of field emission electric propulsion (FEEP) emitters, including recording of the current/voltage characteristic curves and ion beam scanning with electrostatic probes. This work was aimed at collecting reliable, systematic thruster performance data to be used as a basis for the definition of a reference thruster mathematical model (not reported here). Four FEEP emitters with three different slit height values were tested. Thrust produced covered the 1–170 μN range. Repeatability of thruster performance was found to depend on the degree of wetting of the emitter slit and on the presence of glow discharge between the electrodes. The latter represented an undesired effect and was therefore eliminated after the first series of experiments. Wetting, on the contrary, proved to be of the utmost importance. In some cases, thruster performance improved by up to as much as 150% within a few days of the beginning of the test, as a result of enhanced slit wetting.

Introduction

FIELD emission electric propulsion (FEEP), an electrostatic propulsion concept based on field ionization of a liquid metal, is currently the object of great interest in the scientific community because of its unique features: 1 μN to 1 mN thrust range, near instantaneous switch on/switch off capability, and high-resolution throttleability (better than one part in 10^4), which enables accurate thrust modulation in both continuous and pulsed modes. FEEP is presently baselined for several scientific missions onboard drag-free satellites [LISA[1] and OMEGA,[2] multispacecraft gravitational wave detectors; Galileo Galilei (GG)[3] test of the equivalence principle with a small spacecraft], and has been proposed for attitude control and orbit maintenance on commercial small satellites and constellations.[4,5] Developed at Centrospazio, the FEEP system will be flight tested on a Get Away Special canister onboard the Space Shuttle in late 1999.[5]

In the past, FEEP emitter performance data have been collected by several investigators working on emitters with slit lengths ranging from 1 mm to 15 cm.[6–9] In spite of the large number of experiments carried out in several European laboratories, no collection of systematic, parametric tests was available in the literature. In fact, most development efforts were focused on enhancing the current extracted, in an attempt to obtain higher thrust levels. At thrust levels of above a few millinewtons, FEEP has some drawbacks because of the very high specific impulse, which is associated with a very high power-to-thrust ratio. As no established solution was identified to reduce specific impulse, the development of FEEP as a millinewton level thruster was almost terminated in the late 1980s.

The recent shift of perspective on FEEP technology, which now focuses on the very low current capability of this thruster, has drastically changed this situation. At very low thrust levels, i.e., in the micronewton range, the traditional FEEP slit emitter performs best, and its features make it the only candidate for several space applications.[10] Therefore, while engineering refinements to the thruster are still in progress, the concept can be considered to be fully assessed, and serious experimental evaluation of micronewton emitters seems appropriate. This paper presents an overview of the results of the first work carried out to meet this need.

Received Oct. 29, 1997; revision received May 18, 1998; accepted for publication May 21, 1998.

*Project Manager, Via Gherardesca 5. E-mail: s.marcuccio@cpr.it. Member AIAA.

†Research Engineer, Via Gherardesca 5.

‡Director, Via Gherardesca 5; also Professor, Department of Aerospace Engineering, University of Pisa, Pisa, Italy. Member AIAA.

FEEP Thruster

In FEEP emitters, unlike most ion engines, ions are directly extracted from the liquid phase.[11] The thruster can accelerate a large number of different liquid metals or alloys. Cesium is usually selected for its high atomic weight, low ionization potential, low melting point (28.4°C), and good wetting capabilities on the emitter substrate. Specific impulse is in the 4000–10,000 s range, and may be easily adjusted to meet specific mission requirements. Thrust level can be finely tuned, and instantaneous switching capability allows pulsed mode operation and accurate thrust modulation at high bandwidth.[12]

Thrust is produced by exhausting a beam of mainly singly ionized cesium atoms, produced by field evaporation. The emitter module[13] consists of two metallic plates with a small propellant reservoir (Fig. 1). A sharp blade is accurately machined on one side of each plate. A thin layer of Ni is sputter-deposited on the other three sides of one of the plates, to act as a spacer; when the two emitter halves are tightly clamped together, a slit of about 1 μm is left between the blades. Cesium flows through this tiny channel, forming a free surface at the exit of the slit with a radius of curvature in the order of 1 μm. Under a strong electric field generated by the application of a voltage difference between the emitter and an accelerator electrode located directly in front of it, the free surface of the liquid metal approaches a condition of local instability because of the combined effects of the electrostatic force and the surface tension. A series of protruding cusps, or "Taylor cones," are created.[14] When the electric field reaches a value of about 10^9 V/m, the atoms at the tip spontaneously ionize and an ion jet is extracted by the electric field, while the electrons are rejected in the bulk of the liquid. An external source of electrons provides negative charges to maintain global electrical neutrality of the thruster assembly. Mass flow rate is extremely low and requires no control, as the extracted particles are replaced by the capillary actions from the propellant reservoir at a rate sufficient to maintain dynamic equilibrium at the emitter tip. When voltage is removed the capillary force prevents the propellant from pouring out of the slit. A schematic representation of the emitter/accelerator/neutralizer arrangement is shown in Fig. 2.

FEEP Performance Investigation

The test program described in this paper that was carried out in late 1995–early 1996 was aimed at providing the re-

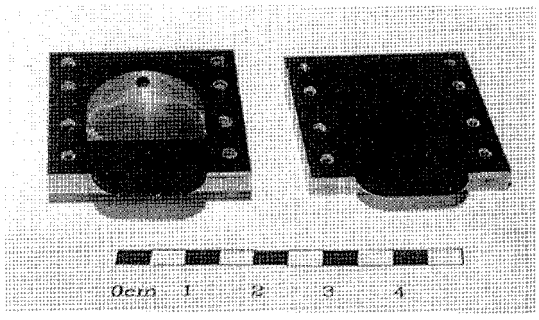

Fig. 1 FEEP emitter.

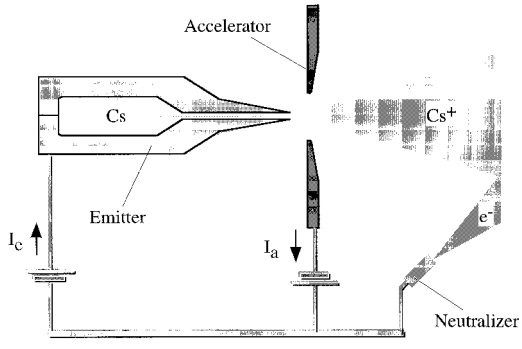

Fig. 2 Schematics of the FEEP thruster.

searchers involved in the development of FEEP, and its potential users, with a set of performance data to be regarded as a reference for this propulsion system. With this in mind, the following thruster features were investigated:

1) *Emission threshold voltage:* Field ionization from the surface of liquid cesium is triggered when a precise threshold value of electric field strength is exceeded at the tip of the Taylor cones. For the purposes of this work, threshold voltage is conventionally defined as the value of electrode total voltage that corresponds to an emission current of 10 μA. At a few tens of volts below threshold, emission is practically negligible.

2) *Emission development in time at first ignition:* The degree of emitter slit wetting by propellant can be estimated by recording the variation in time of the ion current. In fact, wetting may progress very slowly, e.g., when the surfaces of the tips are not perfectly clean, or when the background atmosphere contains contaminants (H_2O, O_2, atomic oxygen). In some cases, wetting develops fully only after several days.

3) *Characteristic curves:* Emitter current, I_e, and accelerator current, I_a, as a function of total voltage, $\Delta V = V_e + V_a$, where V_e is the emitter voltage (positive with respect to ground) and V_a is the absolute value of accelerator voltage (negative with respect to ground). In an ideal situation, emitter current is a function of the total electrode voltage. In practice, the actual distribution of voltage between the electrodes may affect the emission current, as some charge is drained through the accelerator. Power efficiency, η, i.e., the ratio of kinetic power output of the exhausted beam to electrical power input to the thruster, may be easily computed as

$$\eta = \frac{V_e(I_e - I_a)}{V_e I_e + V_a I_a} \tag{1}$$

4) *Ion beam profile:* Knowledge of the ion beam shape is of great practical interest, particularly for thruster–spacecraft integration issues. A convenient method to assess the ion beam shape is the use of single filament electrostatic probes, biased negatively with respect to ground by an external power supply. Positive charges hitting the probe give rise to a small current flow that can be regarded as an indication of the local ion beam characteristics. However, it should be noted that this probing technique provides qualitative information only. The current drained by the probe is a complex function of local ion density, ion velocity magnitude and direction, ambient electron density and temperature, secondary electron emission from the probe itself, and geometrical and physical details of its surface. Moreover, the measure is spatially averaged over the filament length. Therefore, it is not possible to extract quantitative information on the ion beam features from those measurements. A detailed investigation of the FEEP plume requires more sophisticated techniques, such as double-filament Langmuir probing.[15] The latter technique was not adopted in this case because of time and budget constraints. Nevertheless, the single-filament technique gives a quick overview of the overall beam geometry and, therefore, has been extensively used to this end in this work.

Direct thrust measurement was not performed. To date, no thrust stand is available in the micronewton range, although a dedicated thrust balance for micronewton FEEP is under development at Centrospazio.[16] Neglecting the effects of nonideal charge to mass ratio resulting from multiply-charged ions and from charged atom clusters, thrust was therefore calculated using the following relation:

$$T = \sqrt{(2m_{Cs}/e)} I_e V_e^{1/2} = 1.666 \times 10^{-3} I_e V_e^{1/2} \tag{2}$$

where T is thrust in N, $m_{Cs} = 2.207 \times 10^{-25}$ kg is the atomic mass of cesium, $e = 1.602 \times 10^{-19}$ C is the elementary charge, I_e is emission current in amperes, and V_e is emitter voltage in volts. In the following, thrust computed according to Eq. (2) will be referred to as "theoretical thrust." This relation was validated by comparison with measurements made at the European Space Research and Technology Center (ESTEC) in the early 1980s on FEEP emitters in the millinewton range, using a torsion balance.[13] As FEEP thrust depends only on emitted current and electrode voltage, it would seem reasonable that Eq. (2) also holds for the micronewton range. Modified thrust, $\bar{T}$, is defined[13] as

$$\bar{T} = T(\sin \alpha/\alpha)(\sin \beta/\beta) \tag{3}$$

where α and β are the ion beam divergence angles (Fig. 3). Modified thrust takes the thrust reduction resulting from beam divergence into account, in an approximate way. In most cases, modified thrust is about 90% of the theoretical value. Specific impulse, I_{sp}, is given by the following relation:

$$I_{sp} = (1/g_0)\sqrt{2eV_e/m_{Cs}} = 122.3\sqrt{V_e} \tag{4}$$

where I_{sp} is in seconds, $g_0 = 9.81$ m/s^2 is the standard acceleration of gravity, and V_e is in volts. For the voltage range investigated (1 kV ≤ V_e ≤ 9 kV), I_{sp} varies between 3870 and 11,600 s.

Four FEEP emitters were investigated. As a common feature, a slit length of 5 mm (measured along the z direction, Fig. 3) was chosen for all of the emitters. To investigate the role of slit height in determining emitter wetting and emission threshold voltage, three different slit height values were employed (1.2, 1.5, and 1.9 μm). Three Inconel X 750 emitters were made at ESTEC, using the standard manufacturing procedure adopted by the Agency over the last decade. Inconel X 750 is a Ni alloy with 14–17% Cr, easily wetted by cesium, and relatively easy to machine. The fourth unit was a prototype stainless-steel emitter, developed at Centrospazio. AISI 420 stainless steel was selected for its outstanding surface-polishing characteristics, which results in good wetting by the propellant. In all cases, slit spacer deposition and subsequent assembly of the emitter halves were performed at the Department of Electronics of the University of Pisa. Emitters will be referred to as follows: 1) ESA 1: 5 mm slit length, 1.2 μm slit height (test no. 1); 2) ESA 2: 5 mm slit length, 1.9 μm slit height (test no. 2); 3) CS: 5 mm slit length, 1.9 μm slit height

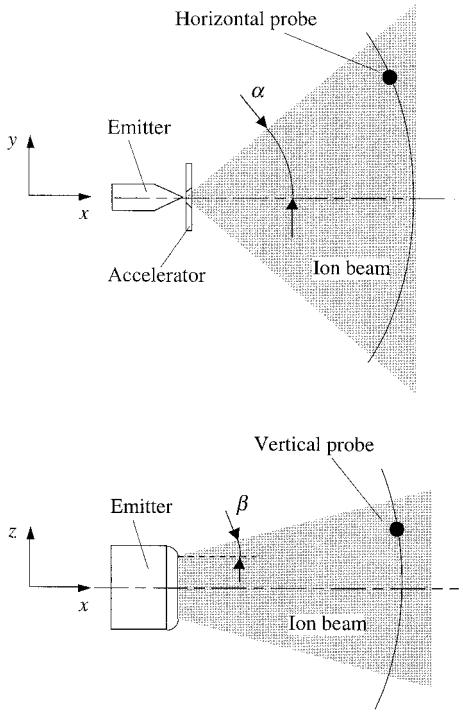

Fig. 3 Ion beam divergence angles and electrostatic probes.

(test no. 3); and 4) ESA 3: 5 mm slit length, 1.4 μm slit height (test no. 4).

Each test included the following phases.

1) A preliminary phase: During this phase the experimental equipment is assembled and mounted on the vacuum chamber flange. Upon attaining the required background pressure, the emitter and feeding system bakeout is performed. The outgassing procedure is accomplished by heating the emitter to 350°C, while the feeding system is heated to 150°C. Bakeout is necessary to degas the water vapor adsorbed by the inner surface of the slit and of the glass siphon, thus preventing the formation of CsOH deposits that would obstruct the flow of cesium towards the slit tip. After the bakeout, the high voltage insulation of all the relevant components is checked.

2) The test phase (which starts with propellant filling): The duration of this phase depends on the number and duration of the thruster tests performed and, consequently, on the number of propellant refillings required.

3) The posttest phase: This phase includes residual propellant evaporation, chamber venting, experimental assembly dismount, thruster dismount, visual inspection, and cleaning.

A neutralizer was not installed, as the electrons extracted by ion impact on the chamber walls automatically provide an adequate neutralizing charge.

Experimental Setup

Centrospazio is equipped with several space simulation facilities. Tests on FEEP thrusters are carried out in the IV1 vacuum chamber, which consists of a stainless-steel vessel with an overall length of 1.8 m and an i.d. of 0.6 m, and is equipped with a turbomolecular pump and a cryopump. The ultimate pressure of the vacuum facility is in the range of 10^{-9} mbar. The chamber pressure and the composition of the residual atmosphere are controlled by pressure-measuring instrumentation, which includes low- and high-vacuum pressure gauges and a quadrupole mass spectrometer for the 0–64 amu range.

The vacuum chamber is equipped with a large experimental flange that bears the emitter–accelerator assembly, an emitter heater (consisting of an etched-foil resistive element laminated between two mica layers), the propellant feeding system, electrical wirings, temperature-monitoring thermocouples, and two motorized electrostatic probes for ion beam scanning. This flange can be removed from the vacuum chamber by an undercarriage. This allows full access to the experimental support plate during assembly and bench-testing.

The propellant feeding system used for experiments consists of a glass siphon containing a sealed ampoule filled with 2.5 g of commercially available, 99.98% pure cesium. The activation of a small electromagnetic gun breaks the seal of the ampoule; cesium is then forced into the terminal capillary part of the siphon by means of a slight overpressure of pure argon. Cesium droplets fall into a funnel connected with the emitter reservoir. Overpressure is released when it can be observed that enough cesium has reached the funnel. The temperature of the system is controlled by means of a resistive heater and a thermocouple, to keep the propellant above its melting point (28.4°C).

Ion beam divergence is measured by a set of two electrostatic wire probes. Each probe consists of a stainless-steel wire with an approximate length of 120 mm and a diameter of 0.8 mm. The horizontal probe provides information on the beam current density distribution in the x–y (vertical) plane, allowing for the measurement of the azimuthal beam divergence angle α. The vertical probe yields the emission profile along the slit (x–z plane) and the lateral divergence angle β, as shown in Fig. 3. The probes are biased at −200 V, with respect to ground, to prevent electron collection. With this arrangement, all positively charged particles contribute to the probe current, and no discrimination is made between fast beam ions and slower charge-exchange ions or multiply charged particles that may be present in the thruster plume. A motorized moveable support system is integrated in the experimental flange with the purpose of positioning the probes. The horizontal probe moves around an axis parallel to the z direction and containing the emitter slit tip, while the vertical probe moves along a circular arc in front of the emitter. The probes are moved by stepper motors driven with a Hewlett Packard 44714A stepper motor controller and a Hewlett Packard 3852A data acquisition /control unit, giving an angular resolution of 0.9 deg. Probe travel ranges are ±53 deg for the horizontal probe and ±66 deg for the vertical probe. Ion beam profiles are obtained by recording the current drained by the probe in each position.

In addition to standard laboratory units, two special high voltage (HV) power supplies were used.

1) A dedicated HV power supply, designed and realized in collaboration with the Department of Electronics of the University of Pisa[17]: This is based on a 10-W switching converter, equipped with a push–pull power stage. This device is capable of delivering high voltage to the accelerator electrode in the form of a square wave with frequency in the range of 0.1–100 Hz and a duty cycle of 10–90%. HV level can be finely adjusted over the 0–8 kV range and a dc bias of several kilovolts can be added.

2) A CAEN Mod. N 570 HV power supply. This device is specially designed for high-energy particle physics detectors. It features a very low ripple (250 mV, peak-to-peak, at full load), very good long-term stability (0.1%) and 1-V resolution in the 0–5 kV range.

Electrical measurements were made using the following instruments:

1) A Keithley 2001 digital multimeter with an accuracy of $\Delta I < 0.05\%$, for the emitter and accelerator currents.

2) A Hewlett Packard 44702B voltmeter and a precision shunt resistor with a resulting accuracy of $\Delta I < 0.05\%$, for the electrostatic probe currents.

Experiment Overview

The following gives a brief report on the four tests performed. For the sake of brevity, only a few examples are reported here from the large amount of data collected. Large day-to-day changes in emitter performance were recorded during the three or four initial days. In all cases, testing was prolonged for a few more days with no further significant variations.

Test No. 1

This test, the first of the series, was aimed at checking the experimental setup, verifying proper operation of the supporting equipment, and refining the test procedures.

Thruster ignition was obtained only three days after propellant feeding. During this period, the emitter temperature was slowly raised to about 80°C, to facilitate wetting by decreasing the viscosity of cesium. Unfortunately, this procedure, which is often used when emission start is not immediate, enhances the evaporation of propellant. The cesium vapor deposits on cold surfaces near the slit and may cause insulation losses at the connections between the thruster and the HV cables. Therefore, some of the currents measured during this test, in particular those at high total voltage, may be slightly higher than actual electrode currents.

Emission started at $V_e = +1.0$ kV, $V_a = -4.0$ kV, i.e., at a very low threshold voltage of 5.0 kV. Figure 4 shows the variation of electrode currents over a span of a few minutes after the first ignition, at constant total voltage. While emission current showed no appreciable variations, the accelerator current increased. At the same time, a glow discharge appeared on the upper part of the accelerator electrode because of the increase in pressure inside the vacuum chamber during the beginning of emission. This is a well-known effect of the vacuum facility: ion beam impingement on the chamber walls induces the release of absorbed gas molecules. In the case of test no. 1, pressure increased from 1×10^{-8} mbar to 3×10^{-6} mbar. This effect vanishes with time: After three days, chamber pressure dropped to 4×10^{-8} mbar, and the glow discharge disappeared.

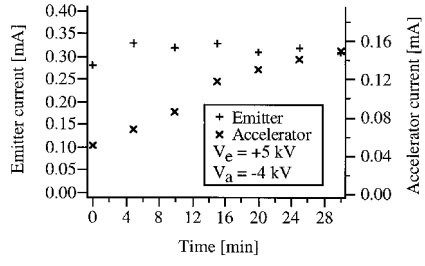

Fig. 4 Variation with time of electrode currents at first ignition (ESA 1).

Figures 5a and 5b show the emitter current vs voltage (characteristic curve) and the current ratio I_a/I_e, respectively, recorded over three different days. In general, accelerator current is the result of different contributions: direct ion beam impingement, which delivers positive charges to the accelerator and induces secondary electron emission, and current losses caused by high ambient pressure, which may result in glow discharge. In optimal background pressure conditions, current losses are negligible. The curves recorded during the first two days show a very high accelerator current because of the glow discharge at the accelerator; the curve recorded on the third day shows a very low accelerator current. The high values of accelerator current and the resulting low values of power efficiency at low emitter voltage are mainly caused by the increase in background pressure, which is more manifest at low V_e. Figure 5c shows modified thrust as a function of electrical power input to the thruster.

Figure 6 shows six ion beam scans recorded on the same day at several emitter voltages. The beam profile is fairly symmetric and divergence angles do not change appreciably with emission current. However, visual inspection after the experiment revealed a number of very small manufacturing irregularities on the accelerator edges, which may have caused a local intensification of the electric field and a consequent irregular ion beam emission. This could explain the quite high divergence angles, $\alpha = 60$ deg and $\beta = 15$ deg, against usual values of $\alpha = 40$ deg and $\beta = 10$ deg.

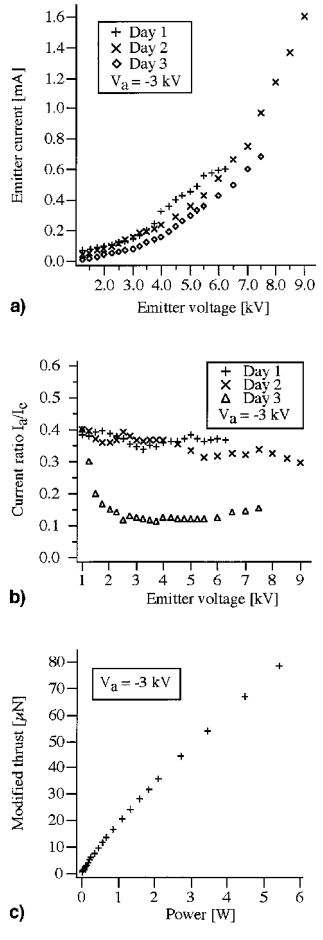

Fig. 5 Characteristic curves (ESA 1): a) emitter current vs emitter voltage, b) current ratio vs emitter voltage, and c) thrust vs power.

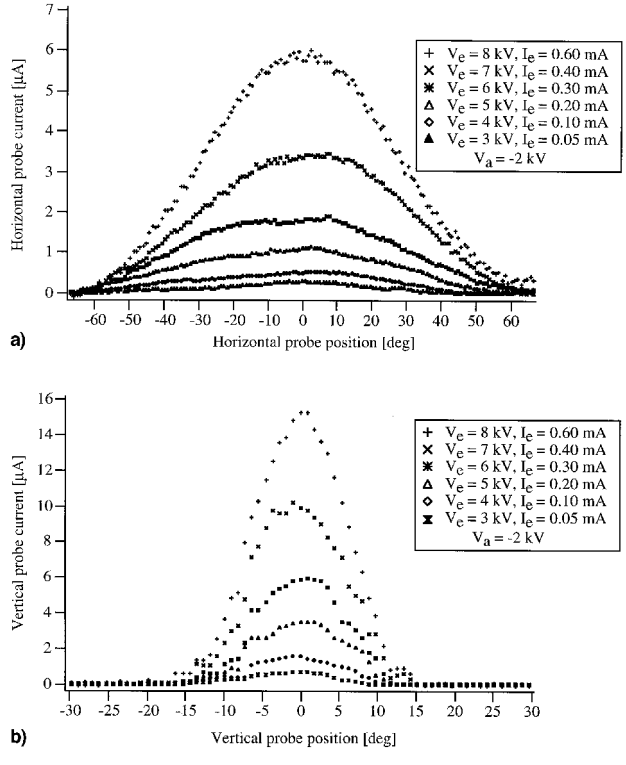

Fig. 6 Ion beam profiles (ESA 1): a) horizontal and b) vertical probes.

Test No. 2

For this test, the accelerator electrode was replaced with a new smoother slit edge electrode. The first ignition of the thruster was immediate, at about 35°C, but at a much higher threshold voltage (about 8.0 kV) than in the previous test. Again, glow discharge could be easily observed on the accelerator electrode after a few minutes of emission, and gradually disappeared during the next days of emitter operation.

Figure 7 shows four characteristic curves, recorded during four different days, clearly indicating a gradual progress of slit wetting: during the fourth day the emission current was 100–150% higher than at the beginning of the test. Current ratio I_a/I_e decreased following the glow discharge extinction. It is interesting to compare Fig. 7 with Fig. 8, which shows a set of characteristic curves recorded when slit wetting was complete and glow discharge absent. Once emission is fully developed, emitter current curves at the same total voltage (Fig. 8a) coincide, regardless of the voltage distribution between the electrodes. A 1 kV decrease in threshold voltage can also be noticed. Lower accelerator voltage (Fig. 8b) results in better power efficiency, as accelerator current is reduced. Thrust vs power is shown in Fig. 8c.

Figure 9 shows ion beam profiles recorded on the same day at equal V_a and different values of V_e. Divergence angles are $\alpha = 40$ deg and $\beta = 15$ deg.

Test No. 3

This test was aimed at evaluating the performance of the first FEEP emitter prototype manufactured at Centrospazio, with a completely new design. Unlike the ESA emitters, the new emitter was designed taking the specific requirements of a micronewton thruster into account. The CS emitter features a small, integrated propellant reservoir, specially shaped for capillarity propellant feeding, an improved emitter-tip contour, and was made using new, semiautomated machining and finishing techniques. Moreover, a new emitter mount and new HV isolators were used.

As expected, this test revealed a number of minor faults, which helped in refining the emitter design. Emitter performance, although not excellent, was very satisfactory for a prototype. Emitter ignition was performed immediately after propellant feeding, without any slit wetting problem, at a threshold voltage of only 5.5 kV. As in the previous tests, after a short period a glow discharge was observed, now located on the isolator between the accelerator and emitter. As a consequence, high total voltage thruster operation was prevented.

Figure 10 shows the characteristic curve at $V_a = -3$ kV and the thrust vs power curve. Regardless of the presence of glow discharge, the I_a/I_e ratio was as low as 10% and power efficiency exceeded 90%. Figure 11 shows rather unusual profiles of the ion beam and high divergence angles, most likely caused

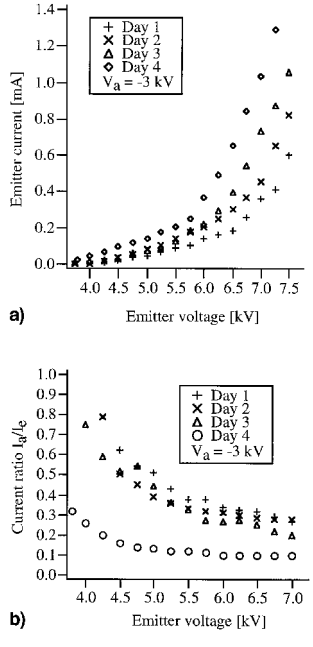

Fig. 7 Characteristic curves (ESA 2) with glow discharge: a) emitter current vs emitter voltage and b) current ratio vs emitter voltage.

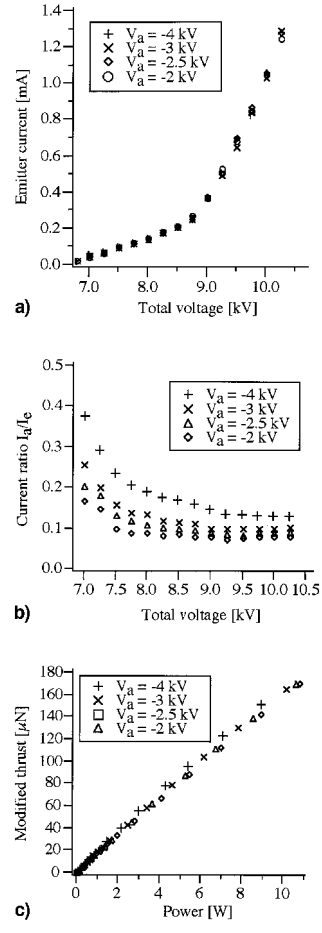

Fig. 8 Characteristic curves (ESA 2) without glow discharge: a) emitter current vs emitter voltage, b) current ratio vs emitter voltage, and c) thrust vs power.

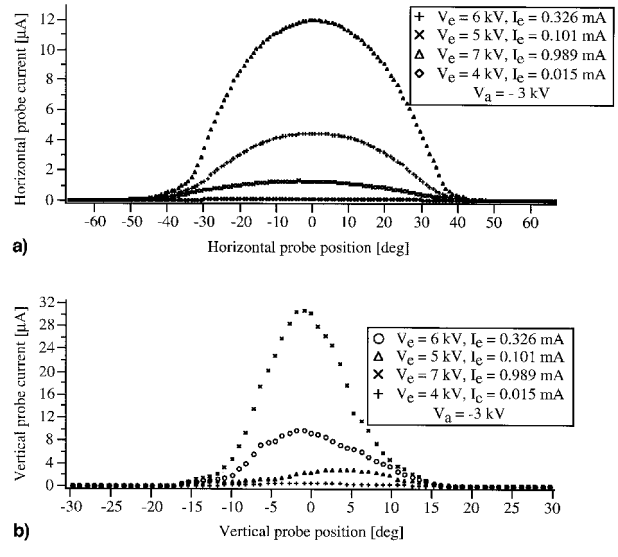

Fig. 9 Ion beam profiles (ESA 2): a) horizontal and b) vertical probes.

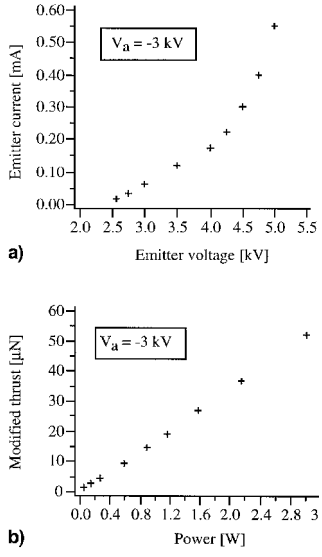

Fig. 10 Characteristic curves (CS): a) emitter current vs emitter voltage and b) thrust vs power.

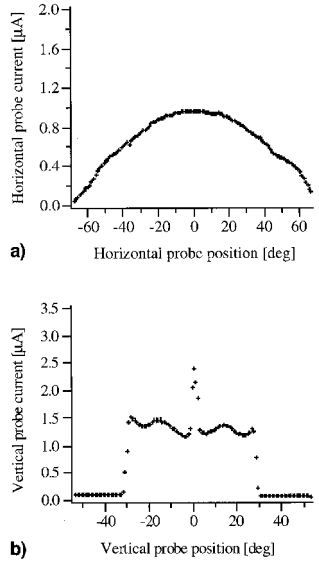

Fig. 11 Ion beam profiles (CS): a) horizontal and b) vertical probes.

by the different emitter geometry resulting from the new manufacturing processes. In particular, the shape of the beam in the x–z plane is very sharp near the edges of the slit, and peaks around the center, which may be a result of a local imperfection of the slit tips.

Test No. 4

Overall performance of ESA 3 was very satisfactory. The thruster was readily ignited after propellant feeding. Figures 12a and 12b show characteristic curves and I_a/I_e curves recorded over three days. Figure 12c shows thrust as a function of power consumption. Slit wetting was satisfactory from the beginning. Initially, the accelerator current was very high, again because of the formation of a glow discharge on the accelerator, and dropped rapidly upon extinction of the discharge, which spontaneously occurred after a period of time. As a consequence, an I_a/I_e ratio as low as 7% and a power efficiency as high as 97% were reached.

Figure 13 shows three ion beam profiles, recorded at fixed accelerator voltage. The beam is very symmetric, with small divergence angles (α is about 40 deg and β is 10 deg). Thrust loss caused by divergence is therefore less than 10%.

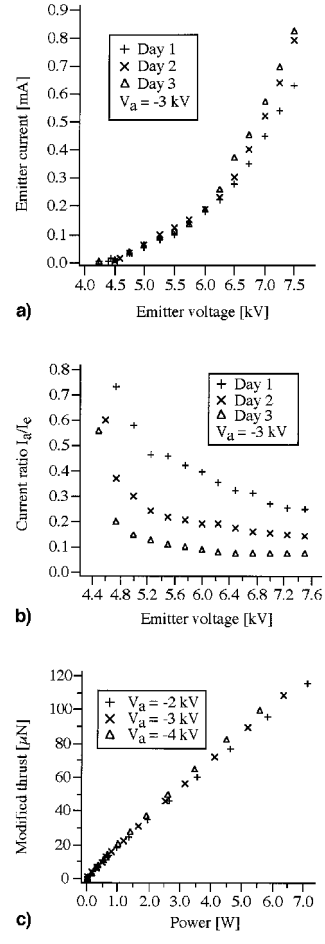

Fig. 12 Characteristic curves (ESA 3): a) emitter current vs emitter voltage, b) current ratio vs emitter voltage, and c) thrust vs power.

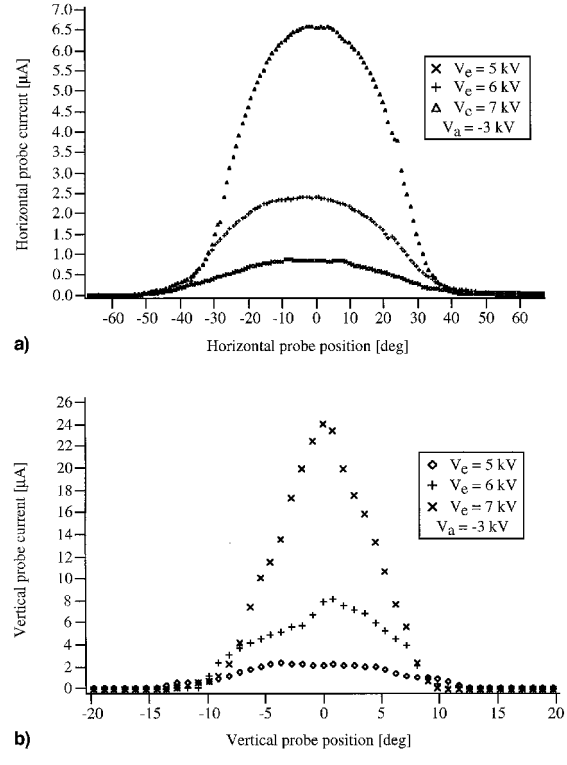

Fig. 13 Ion beam profiles (ESA 3): a) horizontal and b) vertical probes.

Test Results

A major difference between the emitters tested is represented by the threshold voltage, which ranges from 4 kV (ESA 1) to 7.5 kV (ESA 3). Figure 14a shows four characteristic curves, one for each emitter tested during this test campaign. In spite of the testing problems affecting ESA 1 performance, this emitter showed the lowest threshold voltage, even lower than that of a similar 1.2-μm emitter tested at ESTEC in the past.[18] The characteristic curves of ESA 2 and ESA 3 differ only in a shift of the 1.4-μm emitter curve toward higher values of the emitter voltage because of the different threshold voltage. In fact, the current produced by the thruster is essentially a function of the electric field at the surface of the liquid propellant. The same field intensity may be obtained at different values of total voltage, depending on the microscopic details of the emitter tips, and first of all its actual curvature. The influence of other geometrical parameters, such as the interelectrode gap, d, is less marked; for all of the emitters tested, d was set at 0.6 mm to within ±5 μm, i.e., with an error to all intents and purposes that was negligible. The effect of slit height on emitter performance was less marked than expected. In fact, among the ESA emitters, only the 1.2-μm emitter showed a significantly different threshold voltage and characteristic curve shape.

As a first prototype, the CS emitter showed a good overall performance, in spite of isolation problems that limited the total voltage range to about 2.5 kV. The slope of its characteristic curve does not differ from that of ESA 2 and ESA 3. Threshold voltage is much lower, indicating that the slit tips are very sharp, allowing for the same electric field at the propellant surface to be produced at a lower total voltage.

Power efficiency of the three ESA emitters is shown in Fig. 14b. In all cases, very good power efficiency was recorded, exceeding 95% at higher voltages. The recorded CS emitter power efficiency was less satisfactory, because of the isolation loss that impaired the accelerator current measurements. However, thrust performance is very similar for all emitters, as shown in Fig. 14c. From a spacecraft system-level point of view, the differences between the emitters tested look almost negligible, as the involved power consumption (50–60 mW/μN) is very low in all cases. Comparable differences would make a much stronger impact if scaled up to millinewton thrust level.

As shown in Figs. 9 and 13, divergence angles of the best performing emitters (ESA 2 and ESA 3) are quite limited. Future flight models may benefit from the introduction of additional beam-shaping electrodes to further reduce beam divergence.

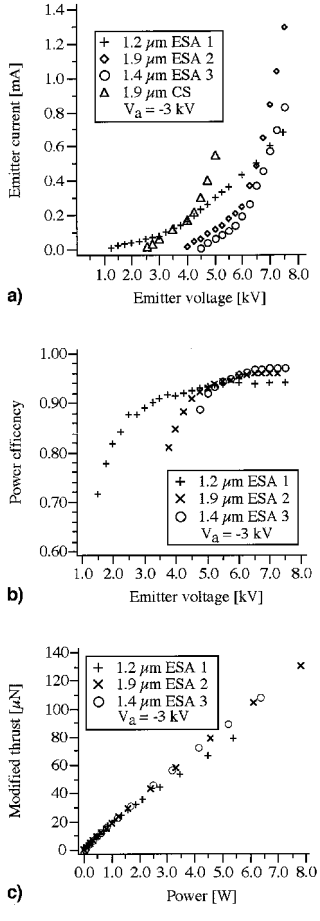

Fig. 14 Summary of tests: a) emitter current vs emitter voltage, b) power efficiency, and c) thrust vs power.

Conclusions

Measured thruster performance confirmed the behavior predicted by extrapolating data of millinewton thrust level field emitters. Repeatability of the tests was very good as long as steady conditions were reached, i.e., as soon as the vacuum chamber wall effects became negligible. Encouraging results were obtained with the new emitter with integrated reservoir, although additional work is needed to solve the HV isolation problems.

Measurements reported in this paper are the first systematic collection of FEEP performance data at a micronewton level. The results of this activity, in particular those of test no. 4, can be assumed as a reference for estimating the performance of a micronewton emitter, and that is, to the purpose of sizing a propulsion system. It should, however, be noted that the performance of a FEEP emitter is strongly dependent on the actual geometry of the slit, and an accurate knowledge of the emitter I/V curves may be obtained only by testing.

Acknowledgments

Part of this work was carried out under an ESTEC contract, with Daimler Benz Aerospace as the Prime Contractor. The suggestions of Hansjörg Klotz of DASA and Marc Weinberger of ESTEC were both useful and appreciated. At Centrospazio, Alberto Loro and Davide Dal Pozzo gave important contributions to the experimental activities.

References

[1]Bender, P., et al., "LISA—Laser Interferometer Space Antenna for the Detection and Observation of Gravitational Waves: Pre-Phase A Report," Max-Planck Institut für Quantenoptik, MPQ 208, Garching, Germany, 1995.

[2]Hellings, R. W., "OMEGA—Orbiting Medium Explorer for Gravitational Astrophysics," Midex Proposal, Jet Propulsion Lab., California Inst. of Technology, Pasadena, CA, 1995.

[3]Nobili, A. M., et al., "Galileo Galilei—GG: Flight Experiment on the Equivalence Principle with Field Emission Electric Propulsion," *Journal of the Astronautical Sciences*, Vol. 43, No. 3, 1995, pp. 219–242.

[4]Marcuccio, S., Giannelli, S., and Andrenucci, M., "Attitude and Orbit Control of Small Satellites and Constellations with FEEP Thrusters," *Proceedings of the 25th Electric Propulsion Conference* (Cleveland, OH), 1997, pp. 1152–1159 (IEPC-97-188).

[5]Marcuccio, S., Genovese, A., and Andrenucci, M., "FEEP Thrusters: Development Status and Prospects," *Proceedings of the 2nd European Spacecraft Propulsion Conference* (Noordwijk, The Netherlands), 1997, pp. 149–153 (ESA SP-398).

[6]Bartoli, C., "A Review of Past and Present Research Studies on Ion Field Emission," *Proceedings of the ESTEC Field Emission Day* (Noordwijk, The Netherlands), 1977, pp. 1–10 (ESA SP-119).

[7]Laurini, D., von Rohden, H., Bartoli, C., and Berry, W., "Field Emission Electric Propulsion (FEEP): Steady and Pulsed Modes of Operation," AIAA Paper 87-1046, May 1987.

[8]Andrenucci, M., Marcuccio, S., Spagli, L., Genovese, A., and Repola, F., "Experimental Study of FEEP Emitter Starting Characteristics," *Proceedings of the 22nd International Electric Propulsion Conference* (Viareggio, Italy), 1991 (IEPC-91-103).

[9]Ciucci, A., Genuini, G., and Andrenucci, M., "Experimental Investigation of Field Emission Electrostatic Thrusters," *Proceedings of the 22nd International Electric Propulsion Conference* (Viareggio, Italy), 1991 (IEPC-91-104).

[10]Saccoccia, G., "Electric Propulsion in Europe: Development and Applications," *Proceedings of the 2nd European Spacecraft Propulsion Conference* (Noordwijk, The Netherlands), 1997, pp. 15–25 (ESA SP-398).

[11]Swanson, L. W., and Kingham, D. R., "On the Mechanism of Liquid Metal Ion Sources," *Applied Physics A*, No. 41, 1986, pp. 223–232.

[12]Klotz, H., Strauch, H., Wolfsberger, W., Marcuccio, S., and Speake, C., "Drag-Free, Attitude and Orbit Control for LISA," *Proceedings of the ESA/ESTEC 3rd International Symposium on Spacecraft Guidance, Navigation and Control*, (Noordwijk, The Netherlands), 1996, pp. 695–702 (ESA SP-381).

[13]Bartoli, C., von Rohden, H., Thompson, S. P., and Blommers, J., "A Liquid Cæsium Field Ion Source for Space Propulsion," *Journal of Physics D: Applied Physics*, Vol. 17, 1984, pp. 2473–2483.

[14]Taylor, G., "Disintegration of Water Drops in an Electric Field," *Proceedings of the Royal Society of London, Series A: Mathematical and Physical Sciences*, Vol. 280, 1964, pp. 383–397.

[15]Marcuccio, S., Genovese, A., and Andrenucci, M., "FEEP Thruster Plume Investigation with Langmuir Probes," *Proceedings of the 24th International Electric Propulsion Conference* (Moscow, Russia), 1995, pp. 649–664 (IEPC-95-98).

[16]Paolucci, F., d'Agostino, L., and Burgoni, S., "Design and Performance Study of a Micro-Newton Thrust Stand for FEEP," *Proceedings of the 2nd European Spacecraft Propulsion Conference* (Noordwijk, The Netherlands), 1997, pp. 465–472 (SP-398).

[17]Genovese, A., Marcuccio, S., De Sio, M., and Andrenucci, M., "Pulsed FEEP: New Experimental Results," *Proceedings of the 24th International Electric Propulsion Conference* (Moscow, Russia), 1995, pp. 643–648 (IEPC-95-97).

[18]Gonzalez, J., Saccoccia, G., and von Rohden, H., "Field Emission Electric Propulsion: Experimental Investigations on Microthrust FEEP Thrusters," *Proceedings of the 23rd International Electric Propulsion Conference* (Seattle, WA), 1993, pp. 1423–1431 (IEPC-93-157).